Accepted Manuscript

Palladium(II) Complexes Supported by a Bidentate *Bis*(secondary)phosphine Linked by Pyridine

Matthew S. Winston, John E. Bercaw

PII: S0020-1693(14)00474-5
DOI: http://dx.doi.org/10.1016/j.ica.2014.08.002
Reference: ICA 16136

To appear in: *Inorganica Chimica Acta*

Received Date: 6 May 2014
Revised Date: 30 July 2014
Accepted Date: 1 August 2014

Please cite this article as: M.S. Winston, J.E. Bercaw, Palladium(II) Complexes Supported by a Bidentate *Bis*(secondary)phosphine Linked by Pyridine, *Inorganica Chimica Acta* (2014), doi: http://dx.doi.org/10.1016/j.ica.2014.08.002

Palladium(II) Complexes Supported by a Bidentate *Bis*(secondary)phosphine Linked by Pyridine

Matthew S. Winston and John E. Bercaw*

Department of Chemistry, California Institute of Technology, Pasadena, CA 91125, United States

Abstract

A series of complexes of the type (PNP-H_2)PdX_2 (X = Cl, Br, I) have been synthesized, where PNP-H_2 is a bis(secondary)phosphine ligand linked by a pyridine, 2,6-(Ph(H)P)$_2$(C_5H_3N). Due to chirality at phosphorus, the parent ligand exists as a mixture of nearly equivalent *rac* and *meso* diastereomers non-interconverting at room temperature. When ligated to Pd(II) halides, however, the diastereomeric ratio is dependent upon the halide. The chloro, bromo, and iodo complexes have been characterized crystallographically. Conformationally similar *meso* diastereomers of each dihalide are roughly C_s symmetric in the solid state, while the *rac* diastereomers (identified only for X = Br, I) show substantially different solid-state conformations.

1. Introduction

Transition metal complexes having tertiary phosphine ligands ($PR^1R^2R^3$), including those with chirality at one or more phosphorus atoms, have been extensively investigated.[1] By contrast, secondary phosphines (PHR^1R^2) and their coordination preferences to transition metals are far less explored,[2] likely due to their toxicity, volatility and pyrophoric nature. Moreover, their syntheses often require the intermediacy of compounds bearing phosphorus protecting groups (boranes, oxides, sulfides, and selenides) for purification that may only be removed under reducing conditions.[3]

Bis(secondary)phosphines in pincer frameworks are even less common, owing to challenges in controlling the reactivity of the phosphorus atom in a many-step synthesis. To our knowledge, only two have been reported. Turculet and coworkers synthesized a xanthene-derived POP-type bis(secondary)phosphine and investigated the coordination of its bis(phosphide) conjugate base to early metals.[4] Our group also prepared a pyridine-linked PNP-type bis(secondary)phosphine (compound 2, below) as a 1:1 mixture of *P*-chiral *meso* and *rac* diastereomers that interconvert at elevated temperatures ($\Delta G^{\ddagger}$ = 18.3 kcal/mol at 110 °C).[5] Because the bis(phosphide) dianion coordinates to potassium and zirconium as a single diastereomer, we were interested in studying the stereochemistry and coordination chemistry of the neutral parent *bis*(secondary)phosphine bound to late metals. Accordingly, we report herein the synthesis and structural characterization of new Pd(II) complexes with the 2,6-$(Ph(H)P)_2(C_5H_3N)$ pincer ligand.

2. Results and discussion

*2.1. Synthesis and Characterization of (meso-PNP-H_2)$PdCl_2$ (**3**-meso).*

S_NAr reaction of K[PHPh] with bis(fluoride) **1** affords an equivalent mixture of **2**-*rac* and **2**-*meso* in 70% yield with diagnostic ^{31}P NMR signals (-44.5 ppm, $^1J_{P\text{-}H}$ = 227 Hz; -43.9, $^1J_{P\text{-}H}$ = 224 Hz) (eq. 1). Treatment of 1:1 **2**-*meso*:**2**-*rac* with $(COD)PdCl_2$ (COD = 1,4-cyclooctadiene) in benzene for 3 h affords a single species by ^{31}P NMR (a doublet at δ 12.0 ppm, $^1J_{P\text{-}H}$ = 378 Hz) (eq. 2).

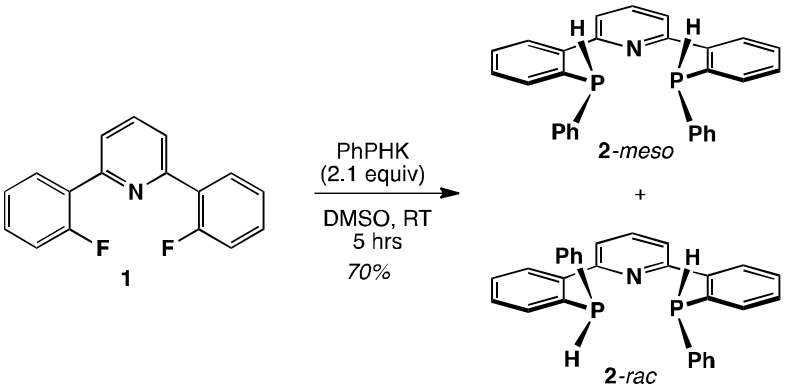

(1)

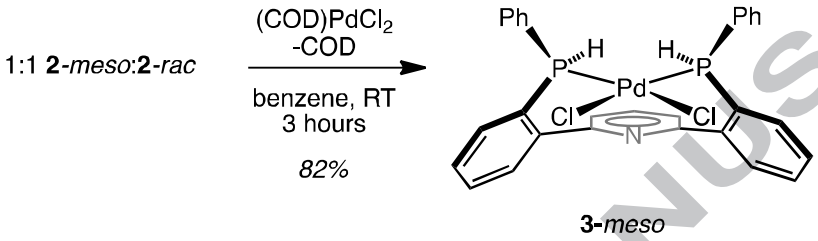

(2)

X-ray analysis of crystals grown from saturated CH_2Cl_2 allowed unambiguous identification of the phosphine stereochemistry (Figure 1). The phosphines are in a *meso* relationship, and the square plane of the Pd(II) is conserved ($\Sigma\angle_{Pd}$ = 360.028(24)°). In the solid-state, **3**-*meso* is roughly C_S-symmetric, with a P-Pd-P bite angle of 91.342(13)°. The Pd-P bonds (2.2319(3) Å and 2.2211(3) Å) are appreciably shorter than the Pd-$PHPh_2$ bond in $[(PHPh_2)(I)Pd(\mu\text{-}PPh_2)]_2$ (2.3289(7) Å),[6] and also shorter by ~0.1 Å than the Pd-P bonds in a series of dimesitylphosphine-supported Pd(II) complexes (Table 1),[7a-7c] although this may be a result of the larger phosphine cone angle. In contrast, the Pd-P bonds in **3**-*meso* are similar to those of more common bidentate ligand-supported dichloride complexes (dppm)$PdCl_2$ (2.242(1) Å),[8a] (dppe)$PdCl_2$ (2.229(2) Å),[8a] and (dppp)$PdCl_2$ (2.247(1) Å).[8b] The solution-state interconversion of **3**-*meso* to its *rac* diastereomer was probed by $^{31}P\{^1H\}$ VT-NMR, but no new signals were observed between -80 °C and 60 °C.

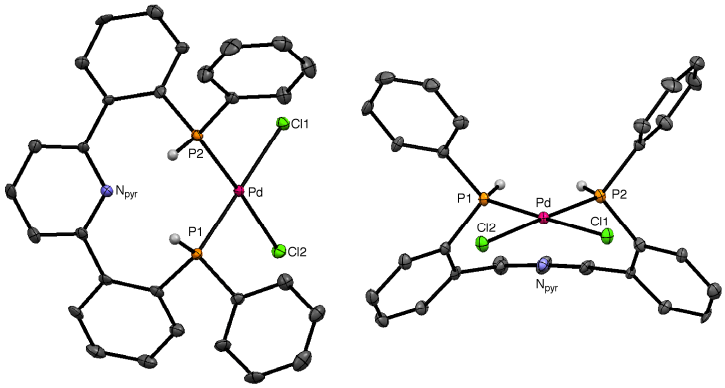

Figure 1. Thermal ellipsoid representation of (*meso*-PNP-H_2)$PdCl_2$ (**3**-*meso*) at the 50% probability level. All C-bound hydrogens have been omitted. Atoms are color coded: carbon (gray), hydrogen (light gray), chlorine (green), nitrogen (blue), palladium (pink), phosphorus (orange). Selected bond lengths (Å) and angles (°): Pd-P1 2.2319(3); Pd-P2 2.2211(3); Pd-Cl1 2.3443(3); Pd-Cl2 2.3614(3); P1-Pd-P2 91.342(13).

*2.2. Synthesis and Characterization of (meso-PNP-H_2)$PdBr_2$ (**4-**meso) and (rac-PNP-H_2)$PdBr_2$* **(4-*rac*).**

Reaction of *trans*-$(MeCN)_2PdBr_2$ with 1:1 **2**-*meso*:**2**-*rac* in benzene for 3 h generates two species in a 5.0:1 ratio (eq. 3). The similarity in NMR signals of the major product to those of the analogous **3**-*meso* (doublet at δ 10.8 ppm in the ^{31}P NMR, $^{1}J_{P\text{-}H}$ = 378 Hz*;* triplet at δ 8.15 ppm in the ^{1}H NMR attributed to the pyridine 4-H) suggest that the *meso*-bound dibromide (**4**-*meso*) is predominate. Therefore, the minor diastereomer (doublet at δ 5.0 ppm in the ^{31}P NMR spectrum, $^{1}J_{P\text{-}H}$ = 411 Hz; triplet at δ 7.93 ppm in the ^{1}H NMR attributed to the pyridine 4-H) is presumably **4**-*rac*. The equilibrium between **4**-*meso* and **4**-*rac* can be probed by ^{1}H VT-NMR. At -60 ℃, only **4**-*meso* is detectable in solution, clearly indicating that it is the enthalpically favored diastereomer. At 40 ℃ and

60 °C, the ratio **4**-*meso*:**4**-*rac* is 4.0:1 and 2.7:1, respectively (ΔH° = 3.5 kcal/mol, ΔS° = -8.3 e.u.).

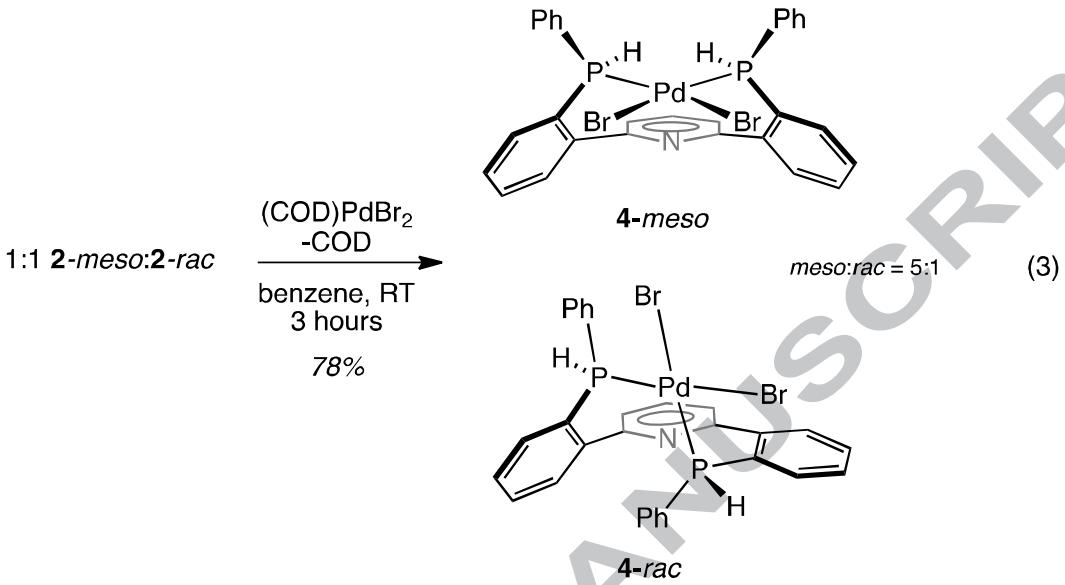

Slow evaporation of a saturated CH_2Cl_2 solution of **4**-*meso*/**4**-*rac* affords both block-shaped and blade-like crystals that crystallize in space group $P2_1/c$. The former crystals analyze as **4**-*meso*, which is essentially isostructural to **3**-*meso* (Figure 2). In the solid state, **4**-*meso* is nearly C_s-symmetric. Pd-P bond lengths vary only slightly from those of its dichloride analogue (2.2328(3) and 2.2452(3) Å) and the Pd(II) center is unambiguously square planar ($\Sigma\angle_{Pd}$ = 360.047(20)°). The Pd-P bond lengths are comparable to those of **4**-*meso* (2.2407(4) and 2.2761(5) Å).

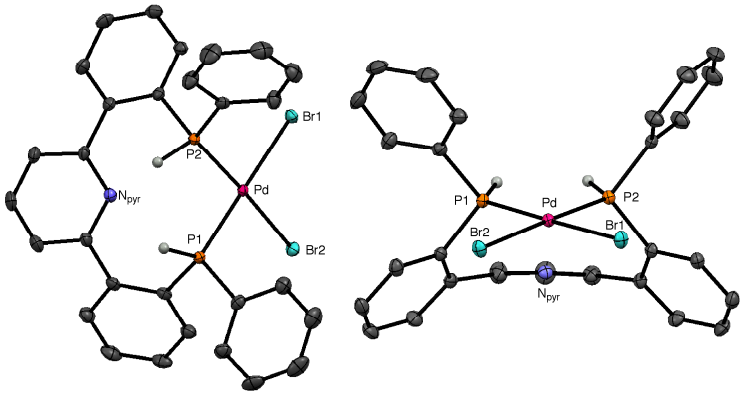

Figure 2. Thermal ellipsoid representation of (*meso*-PNP-H_2)$PdBr_2$ (**4**-*meso*) at the 50% probability level. All C-bound hydrogens have been omitted. Atoms are color coded: carbon (gray), hydrogen (light gray), bromine (turquoise), nitrogen (blue), palladium (pink), phosphorus (orange). Selected bond lengths (Å) and angles (°): Pd-P1 2.2328(3); Pd-P2 2.2452(3); Pd-Br1 2.48284(16); Pd-Br2 2.46995(17); P1-Pd-P2 91.289(13).

On the other hand, both antipodes of the minor diastereomer, **4**-*rac*, crystallize together and exhibit a remarkably different C_1-symmetric geometry in the solid state (the (*S,S)* antipode is shown in Figure 3). The Pd(II) center again is planar ($\Sigma\angle_{Pd}$ = 360.126(25)°), but the *rac* diastereomer of the ligand coordinates with an enlarged bite angle (P1-Pd-P2 = 99.031(17)°), essentially that of (1,1'-bis(diphenylphosphino)ferrocene)($PdCl_2$) (P-Pd-P = 99.07(5)°).[8b] Presumably, the large bite angle arises from a combination of steric pressure from both *P*-bound phenyl rings and the square plane of the metal coordination sphere, as they can no longer avoid each other in space as they do in the *meso* diastereomer.

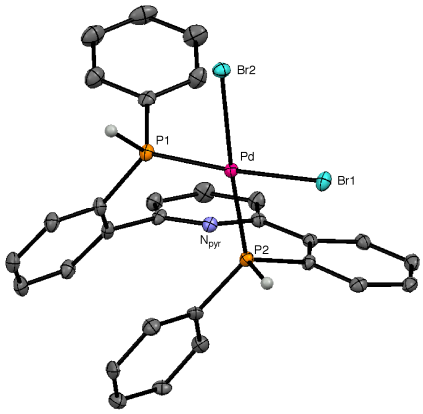

Figure 3. Thermal ellipsoid representation of (*S,S*)-(*rac*-PNP-H_2)$PdBr_2$ (**4**-*rac*) at the 50% probability level. All C-bound hydrogens have been omitted. Atoms are color coded: carbon (gray), hydrogen (light gray), bromine (turquoise), nitrogen (blue), palladium (pink), phosphorus (orange). Selected bond lengths (Å) and angles (°): Pd-P1 2.2407(4); Pd-P2 2.2761(5); Pd-Br1 2.5020(2); Pd-Br2 2.4894(2); P1-Pd-P2 99.031(17).

2.3. Synthesis and Characterization of (meso-PNP-H_2)PdI_2 **(5-***meso***)** *and (rac-PNP-H_2)PdI_2 (***5-***rac)***.***

The reaction of *trans*-$(PPh_3)_2PdI_2$ with 1:1 **2**-*rac*:**2**-*meso* in benzene for 12 h affords two species (eq. 4). Due to overlapping of diastereomer NMR signals at room temperature, an equilibrium ratio between **5**-*meso* and **5**-*rac* cannot be inferred from the spectrum alone. At -20 °C, the signals arising from the 4-H of each pyridine linker are clearly distinguishable, indicating a 1:1.4 ratio of diastereomers. By analogy to the unambiguously assigned **3**-*meso* (doublet at δ 7.6 ppm in the ^{31}P NMR, $^{1}J_{P\text{-}H}$ = 373 Hz*;* triplet at δ 8.13 ppm in the ^{1}H NMR attributed to the pyridine 4-H), the minor product is assigned as **5**-*meso*. The major product (doublet at δ –2.0 ppm in the ^{31}P NMR spectrum, $^{1}J_{P\text{-}H}$ = 416 Hz; triplet at δ 8.00 ppm in the ^{1}H NMR attributed to the pyridine 4-

H) is therefore **5**-*rac*. At -40 °C and -60 °C, the **5**-*meso*:**5**-*rac* ratios are 1:1.3 and 1:1.2, respectively (ΔH^o = 0.4 kcal/mol, ΔS^o = 2.3 e.u). The equilibrium ratio at room temperature, then, is predicted to be 1:1.7.

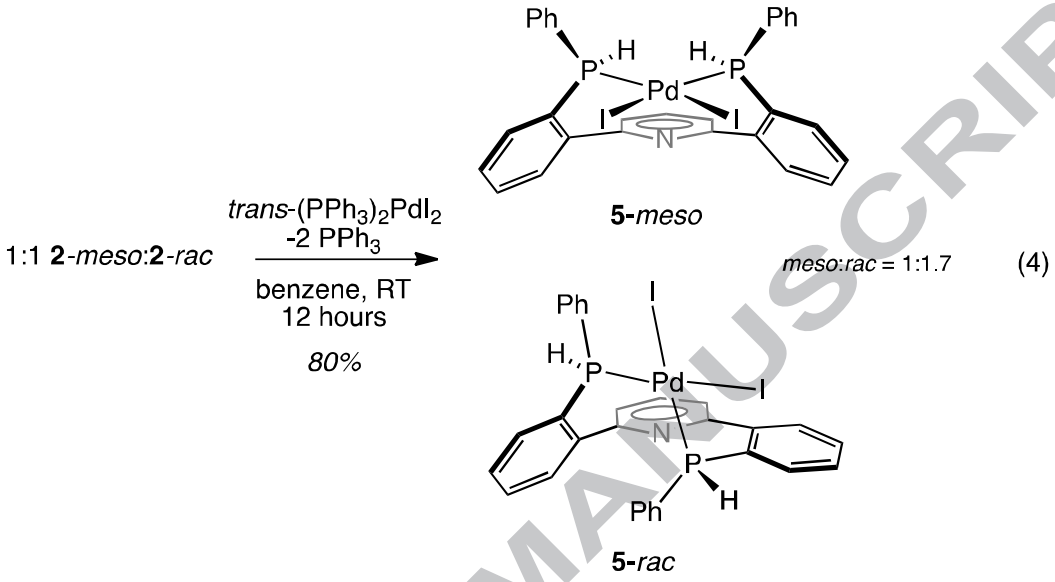

(4)

Slow evaporation of a saturated THF solution of **5**-*meso*/**5**-*rac* gives both orange, blade-like crystals and red, block-shaped crystals. The former crystallize in space group $P\bar{1}$ and analyze as the roughly C_s-symmetric **5**-*meso* (Figure 4). The Pd(II) center is square planar ($\Sigma\angle_{Pd}$ = 361.09(8)°), and the Pd-P bond lengths (2.2515(15) and 2.2546(14) Å) are comparable to those of isostructural **3**-*meso* and **4**-*meso*. The bite angle is slightly acute (P-Pd-P = 87.53(5)°).

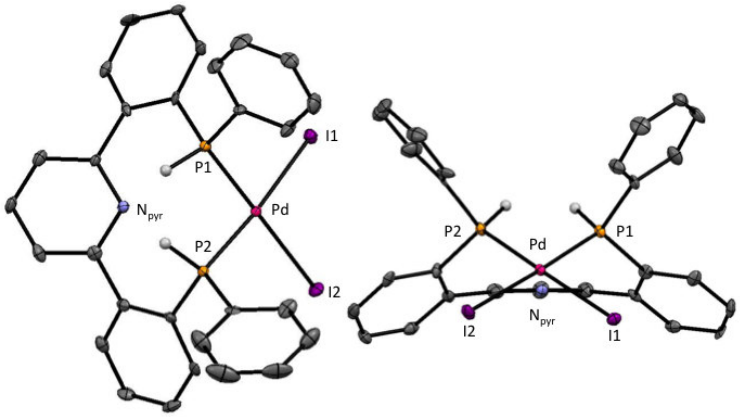

Figure 4. Thermal ellipsoid representation of (*meso*-PNP-H_2)PdI_2 (**5**-*meso*) at the 50% probability level. All C-bound hydrogens have been omitted. Atoms are color coded: carbon (gray), hydrogen (light gray), iodine (purple), nitrogen (blue), palladium (pink), phosphorus (orange). Selected bond lengths (Å) and angles (°): Pd-P1 2.2515(15); Pd-P2 2.2546(14); Pd-I1 2.6387(6); Pd-I2 2.6546(6); P1-Pd-P2 87.53(5).

Both antipodes of major diastereomer **5**-*rac*, on the other hand, crystallize together in space group $P2_1/n$ and are C_1-symmetric in the solid state (the (*R,R*) antipode is shown in Figure 5). The Pd-P bonds are as expected (2.2568(8) and 2.2628(7) Å), and the Pd(II) center is planar ($\Sigma\angle_{Pd}$ = 360.18(4)°). Coordination of the bis(secondary)phosphine ligand to the metal center is less distorted (P-Pd-P = 90.01(3)°) than that of **7**-*rac* in the solid state.

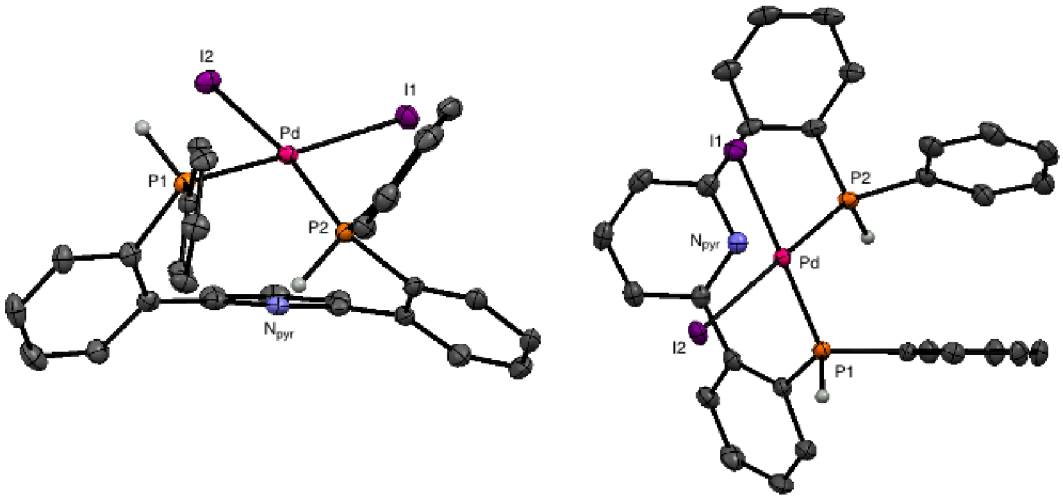

Figure 5. Thermal ellipsoid representation of (*R,R*)-(*rac*-PNP-H_2)PdI_2 (**5**-*rac*) at the 50% probability level. All C-bound hydrogens have been omitted. Atoms are color coded: carbon (gray), hydrogen (light gray), iodine (purple), nitrogen (blue), palladium (pink), phosphorus (orange). Selected bond lengths (Å) and angles (°): Pd-P1 2.2568(8); Pd-P2 2.2628(7); Pd-I1 2.6608(3); Pd-I2 2.6405(3); P1-Pd-P2 90.01(3).

At -40 °C, the $^{31}P\{^1H\}$ NMR signal for **5**-*rac* is unobservable (Figure 6), but the ^1H NMR clearly reveals two species in solution in a 1:1.3 ratio. At -20 °C, the $^{31}P\{^1H\}$ NMR signal attributed to **5**-*rac* appears as a very broad singlet, which sharpens considerably upon warming. This is consistent with the solid-state structure of **5**-*rac*, which indicates two inequivalent phosphorus atoms in each antipode whose signals presumably coalesce upon warming due to fast interconversion on the NMR time scale via a process akin to a flip of the ten-membered chelate ring. Two inequivalent phosphorus atoms should give rise to two singlets in the $^{31}P\{^1H\}$ NMR, although this was not observed at temperatures as low as -60 °C.

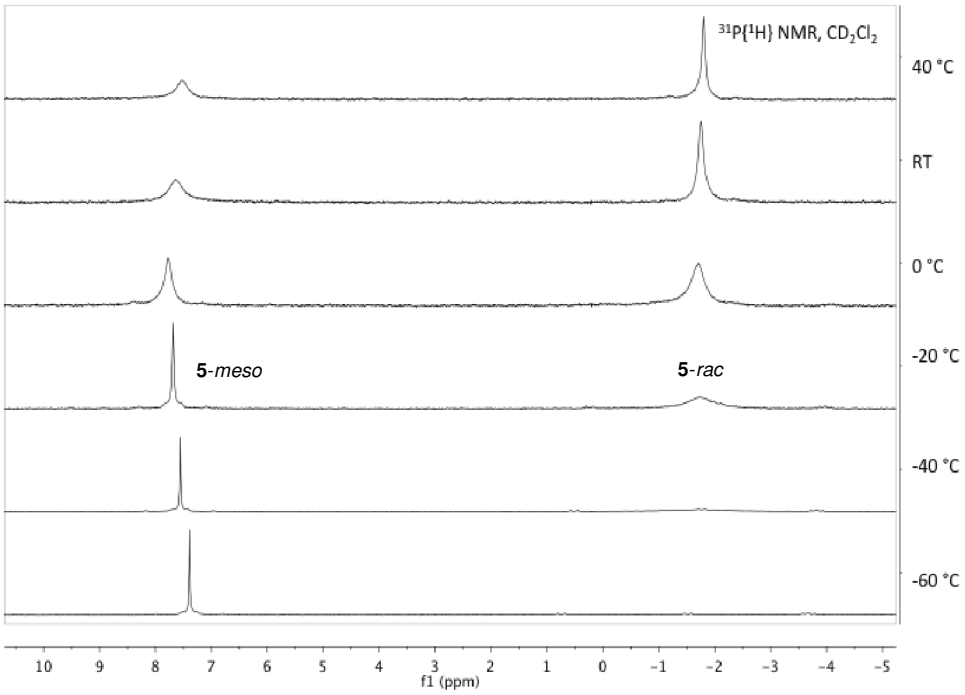

Figure 6. Selected region of variable-temperature $^{31}P\{^{1}H\}$ NMR spectra (202 MHz, CD_2Cl_2) of **5**-*meso* and **5**-*rac*.

3. Conclusions

A series of palladium(II) dihalides with a coordinated bis(secondary)phosphine ligand has been spectroscopically and crystallographically characterized. While the free diastereomeric *rac* and *meso* ligands do not interconvert readily at room temperature, they more rapidly interconvert when bound to Pd(II). While more experiments are necessary to conclusively identify an isomerization mechanism, we speculate that coordination to Pd(II) allows pyridine-assisted deprotonation of the phosphine to afford a zwitterionic Pd(II)-phosphide intermediate; since late metal phosphides have been

shown to have low barriers to pyramidal inversion,[12] a rapid equilibrium between diastereomeric metal complexes can be achieved.

While the *meso*-bound complexes are all roughly C_s-symmetric and their solid state structures are quite similar, the *rac*-bound complexes are more conformationally versatile with **4**-*rac* and **5**-*rac* displaying significant differences in the solid state. This may be a result of reduced steric pressure by the hydrogen substituent on the secondary phosphine ligand, which might influence packing of the *rac* diastereomers in the crystal lattice. Unexpectedly, the thermodynamic diastereomeric ratios of the dihalide complexes are dependent on the nature of the halide ligand. Because these ratios do not deviate in CH_2Cl_2/THF and CH_2Cl_2/TFE mixtures, ground state dipole effects can be largely discounted. Although the conformations of the *rac* ligand are versatile in the solid-state, they bring the coordination plane of the bound Pd(II) closer to the aryl framework than in the *meso*-bound complexes. It is reasonable that destabilizing steric interactions between the *rac* ligand and the halides decrease in the order Cl > Br > I due to increasing Pd-X bond lengths (Cl < Br < I).

Table 1. Structural comparisons of Pd(II) complexes reported in this work and related complexes.

	Complex	P-Pd (Å)	P1-Pd-P2 (°)	reference
this work	(***2**-meso*)$PdCl_2$(**3**-*meso*)	2.2211(3); 2.2319(3)	91.342(13)	-
	(**2**-*meso*)$PdBr_2$(**4**-*meso*)	2.2328(3); 2.2453(3)	91.289(13)	-
	(**2**-*rac*)$PdBr_2$(**4**-*rac*)	2.2407(4); 2.2761(5)	99.031(17)	-
	(**2**-*meso*)PdI_2(**5**-*meso*)	2.2515(15); 2.2546(14)	87.53(5)	-
	(**2**-*rac*)PdI_2(**5**-*rac*)	2.2568(8); 2.2628(7)	90.01(3)	-
secondary phosphines	[Pd(dppe)(**Mes_2PH**)(Ph)]BF_4	2.3446(16)	-	7a
	[Pd(**PPh_2H**)(I)(μ-PPh_2)]$_2$	2.2901(7); 3.6400(7)	72.08(3)	6
	trans-(Mes_2PH)$_2PdCl_2$	2.3057(7); 2.3057(7)	180	7b
	$Pd(Ph_2PH)_4$	2.3213(6)	-	7c
	[$Pd(Ph_2PH)_4$]$(BF_4)_2$	2.340(3)	-	7c
tertiary phosphines	(dppm)$PdCl_2$	2.234(1); 2.250(1)	72.68(3)	8a
	(dppe)$PdCl_2$	2.233(2); 2.226(2)	85.82(7)	8a
	(dppp)$PdCl_2$	2.244(1); 2.249(1)	90.58(5)	8b
	(dppf)$PdCl_2$	2.283(1); 2.301(1)	99.07(5)	8b

Mes = 2,4,6-$(CH_3)_3C_6H_2$; dppm = 1,1-bis(diphenylphosphino)methane; dppe = 1,2-bis(diphenylphosphino)ethane; dppp = 1,3-bis(diphenylphosphino)propane; dppf= 1,1'-bis(diphenylphosphino)ferrocene

4. Experimental Methods

4.1. General Considerations and Instrumentation.

All air- and moisture-sensitive compounds were manipulated using standard high vacuum and Schlenk techniques or manipulated in a glovebox under a nitrogen atmosphere using degassed solvents. All solvents were dried over sodium benzophenone ketyl and stored over titanocene dihydride where compatible or dried by the method of Grubbs.[9] All NMR solvents were purchased from Cambridge Isotopes. Benzene-d_6 was dried over sodium benzophenone ketyl, while CD_2Cl_2 was dried over CaH_2 and stored over molecular sieves. All other chemicals were used as received. $(COD)PdCl_2$ was purchased from Strem Chemical. $(MeCN)_2PdBr_2$[10] and $(PPh_3)_2PdI_2$[11] were prepared according to literature procedure. Ligand **2** was prepared as described in Chapter 1. ^1H, ^{13}C, ^{31}P, and ^{19}F NMR spectra were recorded on Varian Mercury 300 or Varian INOVA-500 spectrometers and unless otherwise indicated at room temperature. Chemical shifts are reported with respect to internal solvent: 7.16 and 128.38 ppm (C_6D_6); 5.32 and 53.84 ppm (CD_2Cl_2) for ^1H and ^{13}C data. ^{31}P chemical shifts are reported with respect to an external 85% H_3PO_4 reference (0 ppm).

4.2. Synthesis and Characterization.

(2-*meso*)$PdCl_2$ (3-*meso*). To a vial equipped with a stirbar and charged with $(COD)PdCl_2$ (32.5 mg, 0.114 mmol, 1.00 equiv) was added benzene (4.0 mL). A benzene solution (1 mL) of **2** (51.5 mg, 0.115 mmol, 1.01 equiv) was added dropwise. A pink suspension formed immediately, which was stirred for 3 hours. After filtering the suspension, the solid was washed with benzene (2 mL), Et_2O (2 mL), then pentane (2 mL), then dried *in vacuo* to afford 71.2 mg of **3-***meso* as an off-white solid in 82% yield. **3-***meso* is slightly soluble in chlorinated solvents, THF, and MeCN. Crystals suitable for x-ray diffraction analysis were grown by slow evaporation of CH_2Cl_2 at room temperature.

^{1}H NMR (500 MHz, CD_2Cl_2) δ: 5.89 (dd, J_1 = 392.4 Hz, J_2 = 31.3 Hz, 2H, ArP*H*(C_6H_5)-Pd), 7.47 (m, 6H), 7.54 (dd, J_1 = 8.2 Hz, J_2 = 6.3 Hz, 2H), 7.62 (m, 4H), 7.73 (dd, J_1 = 13.1 Hz, J_2 = 7.8 Hz, 2H), 7.80 (d, J = 7.8 Hz, 2H), 8.06 (dd, J_1 = 12.7 Hz, J_2 = 7.7 Hz, 4H), 8.14 (t, J = 7.9 Hz, 1H). ^{13}C NMR (126 MHz, CD_2Cl_2) δ: 123.8 (s), 125.3 (s), 125.8 (s), 126.4 (s), 126.8 (s), 129.1 (at, J_1 = J_2 = 11.0 Hz), 130.9 (d, J = 8.2 Hz), 131.9 (s), 132.4 (s), 136.6 (dd, J_1 = 20.8 Hz, J_2 = 10.0 Hz), 139.8 (s), 143.0 (s), 158.4 (s). ^{31}P{^{1}H} NMR (202 MHz, CD_2Cl_2) δ: 12.0 (s). Anal. Calcd. for $C_{29}H_{23}Cl_2NP_2Pd$: C, 55.75; H, 3.71; N, 2.24. Found: C, 55.31; H, 3.55; N, 2.20.

(2-*meso*)$PdBr_2$ (4-*meso*) and **(2-*rac*)$PdBr_2$ (4-*rac*).** To a vial equipped with a stirbar and charged with $(MeCN)_2PdBr_2$ (38.6 mg, 0.111 mmol, 1.00 equiv) was added benzene (4 mL). A benzene solution (1 mL) of **2** (50.0 mg, 0.112 mmol, 1.01 mmol) was added dropwise. After 30 minutes, a light yellow suspension persisted. The reaction was stirred for 3 hours. After filtering the suspension, the solid was washed with benzene (2 mL), Et_2O (2 mL), and pentane (2 mL), then dried *in vacuo* to afford 60.0 mg of **4**-*meso*/**4**-*rac* as a yellow solid in 78% yield. Crystals suitable for x-ray diffraction analysis were grown by slow evaporation of CH_2Cl_2 at room temperature. Due to overlapping signals in the ^{1}H NMR, full spectroscopic characterization of **4**-*rac* could not be obtained. Full characterization spectra were carried out at -60 ℃ to ensure the **4-***meso*/**4**-*rac* equilibrium lies toward >95% **4**-*meso*. ^{1}H NMR (500 MHz, CD_2Cl_2) δ: 5.96 (dd, J_1 = 397.4 Hz, J_2 = 34.6 Hz, 2H, ArP*H*(C_6H_5)-Pd), 7.45 (m, 6H), 7.54 (t, J = 7.5 Hz, 2H), 7.58 (dd, J_1 = 7.2 Hz, J_2 = 4.0 Hz, 2H), 7.63 (t, J = 7.5 Hz, 2H), 7.73 (dd, J_1 = 12.0 Hz, J_2 = 7.9 Hz, 2H), 7.80 (d, J = 7.9 Hz, 2H), 8.00 (dd, J_1 = 13.1 Hz, J_2 = 7.5 Hz, 4H), 8.15 (t, J = 7.9 Hz, 1H). ^{13}C NMR (126 MHz, CD_2Cl_2) δ: 124.2 (s), 125.8 (s), 126.3 (s), 127.3 (s), 127.7 (s), 129.2 (m), 131.2 (at, J_1 = J_2 = 4.0 Hz), 132.2 (s), 132.5 (s), 136.9 (m), 139.9 (s), 143.3

(s), 158.6 (s). $^{31}P\{^{1}H\}$ NMR (202 MHz, CD_2Cl_2) δ: 11.1 (s). Anal. Calcd. for $C_{29}H_{23}Br_2NP_2Pd$: C, 48.81; H, 3.25; N, 1.96. Found: C, 49.07; H, 3.33; N, 2.11.

(2-*meso*)PdI$_2$ (5-*meso*) and **(2-*rac*)PdI$_2$ (5-*rac*).** To a vial equipped with a stirbar and charged with $(PPh_3)_2PdI_2$ (70.6 mmol, 0.080 mmol, 1.00 equiv) was added benzene (3 mL). A benzene solution (1 mL) of **2** (36.1 mg, 0.081 mmol, 1.01 equiv) was added dropwise. A clear dark orange solution formed, which became an orange suspension after 1 hour. After 12 hours stirring at room temperature, the suspension was filtered. The orange solid was washed with benzene (3 mL), Et_2O (5 mL), and pentane (5 mL), then dried *in vacuo* to afford 51.2 mg of **5**-*meso*/**5**-*rac* as a powder in 80% yield. NMR analysis reveals two isomers in about 1:1.5 ratio. **5**-*meso*/**5**-*rac* is slightly soluble in benzene, but dissolves readily in chlorinated solvents and THF. Crystals were grown from a saturated solution in THF. ^{1}H NMR (500 MHz, CD_2Cl_2) δ: 6.11 (dd, J_1 = 381.2 Hz, J_2 = 30.7 Hz, ArP*H*(C_6H_5)-Pd *minor isomer*), 6.99 (dd, J_1 = 416.2 Hz, J_2 = 10.8 Hz, ArP*H*(C_6H_5)-Pd *major isomer*)[8], 7.21 (t, J = 7.5 Hz), 7.30 (dd, J_1 = 11.6 Hz, J_2 = 7.9 Hz), 7.41 (m), 7.52 (m), 7.58 (m), 7.62 (d, J = 7.9 Hz), 7.66 (m), 7.76 (d, J = 7.9 Hz), 7.97 (m), 8.00 (t, J = 8.0 Hz), 8.11 (t, J = 7.8 Hz). ^{13}C NMR (126 MHz, CD_2Cl_2) δ: 124.5 (s), 124.9 (s), 125.6 (s), 126.0 (s), 126.8 (s), 127.2 (s), 129.0 (m), 131.3 (m), 131.7 (s), 132.1 (d, J = 8.5 Hz), 132.4 (s), 132.5 (s), 134.7 (d, J = 10.0 Hz), 135.5 (s), 136.9 (m), 139.1 (s), 139.7 (s), 145.3 (d, J = 10.23 Hz), 157.6 (s). $^{31}P\{^{1}H\}$ NMR (202 MHz, CD_2Cl_2) δ: -2.0 (s), 7.6 (s). ^{31}P NMR (202 MHz, CD_2Cl_2) δ: -2.0 (d, J = 415.5 Hz), 7.6 (d, J = 373.2 Hz). Anal. Calcd. for $C_{29}H_{23}I_2NP_2Pd$: C, 43.12; H, 2.87; N, 1.73. Found: C, 43.09; H, 2.84; N, 1.55.

4.3. Variable-Temperature NMR.

All variable-temperature NMR experiments were performed on a Varian INOVA-500 spectrometer. In a glovebox, an oven-dried J. Young NMR tube was charged with 5-10 mg of analyte and 1.2 mL of CD_2Cl_2 was added. The desired temperature of the NMR probe was set, and after reaching said temperature, the temperature of the tube was allowed to stabilize for 15 minutes before acquiring a spectrum.

4.4. X-Ray Crystal Data: General Procedure.

Crystals grown from CH_2Cl_2 or THF (**3**-*meso*, **4**-*meso*, **4**-*rac,* **5-***meso*, **5**-*rac*) were removed quickly from a scintillation vial to a microscope slide coated with Paratone N oil. Samples were selected and mounted on a glass fiber with Paratone N oil. Data collection was carried out on a Bruker KAPPA APEX II diffractometer with a 0.71073 Å MoKα source. The structures were solved by direct methods. All non-hydrogen atoms were refined anisotropically.

Acknowledgements

The Bruker KAPPA APEXII X-ray diffractometer was purchased via an NSF CRIF:MU award to the California Institute of Technology, CHE-0639094. We gratefully acknowledge the support of the KAUST Center-In-Development at King Fahd University of Petroleum and Minerals (Dhahran, Saudi Arabia) and the USDOE Office of Basic Energy Sciences (Grant No. DE-FG03-85ER13431).

Appendix A. Supplementary Material

Supplementary information associated with this article, including .CIF files and tables for all crystallographically characterized compounds, can be found online at XXXXXXXXX.

References

1. a) Tolman, C. A. *Chem. Rev.* **1977,** *77*, 313. b) Morales-Morales, D.; Cramer, R. E.; Jensen, C. M. *J. Organomet. Chem.* **2002**, *654*, 44. c) Medici, S.; Gagliardo, M.; Williams, S. B.; Chase, P. A.; Gladiali, S.; Lutz, M.; Spek, A. L.; van Klink, G. P. M.; van Koten, G. *Helv. Chim. Acta.* **2005**, *88*, 694.

2. a) Jiang, X.; Minnaard, A. J.; Hessen, B.; Feringa, B. L.; Duchateau, A. L. L.; Andrein, J. G. O.; Boogers, J. A. F.; de Vries, J. G. *Org. Lett.* **2003**, *5*, 1503. b) Ackermann, L.; Kapdi, A. R.; Schulzke, C. *Org. Lett.* **2010**, *12* , 2298.

3. a) Peters, G. *J. Am. Chem. Soc.* **1960**, *82*, 4752. b) Gusarova, N. K.; Malysheva, S. F.; Belogorlova, N. A.; Sukhov, B. G.; Trofimov, B. A. *Synthesis*, **2007**, *18*, 2849. c) Imamoto, T.; Kusumoto, T.; Suzuki, N.; Sato, K. *J. Am. Chem. Soc.* **1985**, *107*, 5301. d) Imamoto, T.; Oshiki, T.; Onozawa, T.; Kusumoto, T.; Sato, K. *J. Am. Chem. Soc.* **1990**, *112*, 5244. e) Wolfe, B.; Livinghouse, T. *J. Am. Chem. Soc.* **1998**, *120*, 5116. f) Berthod, M.; Favre-Réguillon, A; Mohamad, J.; Mignani, G.; Docherty, G.; Lemaire, M. *Synlett*, **2007**, *10*, 1545. g) Petit, C.; Favre-Réguillon, A.; Mignani, G.; Lemaire, M. *Green Chem.*, **2010**, *12*, 326.

4. Turculet, L.; McDonald, R. *Organometallics* **2007**, *26*, 6821.

5. Winston, M. S.; Bercaw, J. E. *Organometallics* **2010**, *29*, 6408.

6. Zhuravel, M. A.; Moncarz, J. R.; Glueck, D. S. *Organometallics* **2000**, *19*, 3447.

7. a) Zhuravel, M. A.; Grewal, N. S.; Glueck, D. S. *Organometallics* **2000**, *19*, 2882. b) Pelczar, E. M.; Nytko, E. A.; Zhuravel, M. A.; Smith, J. R.; Glueck, D. S.; Sommer, R.; Incarvito, C. D.; Rheingold, A. L. *Polyhedron* **2002**, *21*, 2409. c) Leoni, P.; Marchetti, F.; Papucci, S.; Pasquali, M. *J. Organomet. Chem.* **2000**, *593-594*, 12.

8. a) Steffen, W. L.; Palenik, G. J. *Inorg. Chem.* **1976**, *15*, 2432. b) Hayashi, T.; Konishi, M.; Kobori, Y.; Kumada, M.; Higuchi, T.; Hirotsu, K. *J. Am. Chem. Soc.* **1984**, *106*, 158.

9. Pangborn, A. B.; Giardello, M. A.; Grubbs, R. H.; Rosen, R. K.; Timmers, F. J. *Organometallics* **1996**, *15*, 1518.

10. Tan, E. H. P.; Lloyd-Jones, G. C.; Harvey, J. N.; Lennox, A. J. J.; Mills, B. M. *Angew. Chem., Int. Ed.* **2011**, *50,* 9602.

11. Hahn, F. E.; Luegger, T.; Beinhoff, M. *Z. Naturforsch. B.* **2004**, *59*, 196.

12. Rogers, J. R.; Wagner, T. P. S.; Marynick, D. S. *Inorg. Chem.* **1994**, *33*, 3104.

Complex	Pd-P (Å)	P1-Pd-P2 (°)	reference	
(**2-***meso*)$PdCl_2$ (**3**-*meso*)	2.2211(3); 2.2319(3)	91.342(13)	this work	
(**2-***meso*)$PdBr_2$ (**4**-*meso*)	2.2328(3); 2.2453(3)	91.289(13)	this work	
(**2-***rac*)$PdBr_2$ (**4**-*rac*)	2.2407(4); 2.2761(5)	99.031(17)	this work	
(**2-***meso*)PdI_2 (**5**-*meso*)	2.2515(15); 2.2546(14)	87.53(5)	this work	
(**2-***rac*)PdI_2 (**5**-*rac*)	2.2568(8); 2.2628(7)	90.01(3)	this work	
[Pd(dppe)(**Mes_2PH**)(Ph)]BF_4	2.3446(16)	-	7a	secondary phosphines
[Pd(**PPh_2H**)(I)(μ-PPh_2)]$_2$	2.2901(7); 3.6400(7)	72.08(3)	6	
trans-(Mes_2PH)$_2PdCl_2$	2.3057(7); 2.3057(7)	180	7b	
$Pd(Ph_2PH)_4$	2.3213(6)	-	7c	
[$Pd(Ph_2PH)_4$]$(BF_4)_2$	2.340(3)	-	7c	
(dppm)$PdCl_2$	2.234(1); 2.250(1)	72.68(3)	8a	tertiary phosphines
(dppe)$PdCl_2$	2.233(2); 2.226(2)	85.82(7)	8a	
(dppp)$PdCl_2$	2.244(1); 2.249(1)	90.58(5)	8b	
(dppf)$PdCl_2$	2.283(1); 2.301(1)	99.07(5)	8b	

Mes = 2,4,6-$(CH_3)_3C_6H_2$; dppm = 1,1-bis(diphenylphosphino)methane;
dppe = 1,2-bis(diphenylphosphino)ethane;
dppp = 1,3-bis(diphenylphosphino)propane; dppf= 1,1'-bis(diphenylphosphino)ferrocene

Graphical abstract

A series of complexes of the type (PNP-H_2)PdX_2 (X = Cl, Br, I) have been synthesized, where PNP-H_2 is a bis(secondary)phosphine ligand linked by a pyridine, 2,6-(Ph(H)P)$_2$(C_5H_3N). Due to chirality at phosphorus, the parent ligand exists as a mixture of nearly equivalent *rac* and *meso* diastereomers non-interconverting at room temperature.

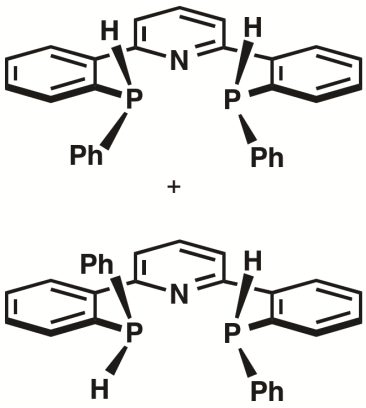

L_2PdX_2

-2 L

(***meso*-PNP-H_2)PdX_2**

+

(***rac*-PNP-H_2)PdX_2**

X	*meso:rac*
Cl	1 : 0
Br	5 : 1
I	1 : 1.7